Application of Volterra Series to the Problem of Self-Oscillating Mixer

Siou Teck Chew, *Student Member, IEEE*, and Tatsuo Itoh, *Fellow, IEEE*

Abstract—**A new approach to the nonlinear problem of self-oscillating mixer has been investigated using Volterra series. The circuit under consideration is first converted into a one-port network. The input and coupling impedances of various ports are represented by Volterra kernels generated by nonlinear current method. Advantage of this approach is that the phase relationships among signals are not required for the analysis. Also, no stability criterion testing is needed to ensure convergence to the correct solution numerically. It is computationally efficient and mathematically simple, yet reasonably accurate. Measured results with respect to RF frequency and power show good agreement with that calculated.**

I. Introduction

SELF-OSCILLATING MIXER (SOM) has been an interesting problem in nonlinear circuit analysis. Being an oscillator by nature, it is an autonomous system that finds its own oscillation frequency, power level, and harmonic contents. However, unlike a free-running oscillator, SOM functions as a mixer in the presence of a RF signal. This RF signal influences the oscillation properties and participates in the frequency conversion with the oscillating signal to generate the IF signal.

There are numerous papers reported on the design of SOM. However, they are mainly empirical and experimental in nature, and involved with two-terminal devices [1]–[4]. Theoretical prediction of the SOM for three-terminal devices is limited. An approximation of the SOM conversion gain was made using closed-form equation derived from an active MESFET mixer (not self-oscillating in nature) [2]. Kipnis and Khanna have simulated a SOM using a BJT with the time-domain large-signal method [5]. However, special considerations for the time step and convergence of the numerical method must be taken for high Q circuit. Rizzoli and Neri applied harmonic balance method, using a Newton-iteration based algorithm, to a FET SOM [6]. But, Jacobian matrix must be computed and Fourier transform must be performed, as required by generic harmonic balance technique. Endo and Chua has proposed analysis of quasi-periodic oscillation problem using Volterra series [7]. However, it is analytical in nature.

Volterra series has been demonstrated to be an efficient simulation tool for nonlinear circuits and systems [7]–[11]. It is commented by [6] that the Volterra kernels are cumbersome to compute. Analytical derivations of these kernels are limited to the first few orders, resulting in its incapability to deal with strong nonlinearity. This also renders the method not suitable for CAD.

In this paper, a new approach is proposed using Volterra series to the SOM problem. The approach is simple mathematically and efficient computationally, yet sufficiently accurate in the prediction of the SOM performance. Restriction of Volterra series mentioned above will be resolved. The proposed approach is an adaptation of the analysis proposed by Cheng and Everard [11] for the free-running oscillator. Phase relationship among signals and stability criterion are not required for the numerical analysis. It must be stressed at this point that the purpose of this paper is to present a new simulation approach for this class of problem and not to design a SOM with optimal conversion gain.

II. Theory

As in [11], the circuit under analysis is first converted into a one-port network by making a break in the circuit, as shown in Fig. 1(a). Z_{IN}, the input impedance looking into that port is expected to be zero for all frequencies under steady state condition. To determine Z_{IN}, a current source with an assumed frequency, ω_0 is attached to the port, as shown in Fig. 1(b). This current source has an ideal frequency-dependent source impedance, Z_S connected in parallel. Z_S assumes an infinite value (open circuit) at the excitation frequency, ω_0 but zero value (short circuit) at all other frequencies (RF, harmonics of RF and oscillating signals, and mixed products).

With a small current excitation, Z_{IN} is the small-signal input impedance and is expected to have negative resistance over a band of frequencies. As the current level increases, Z_{IN} is expected to change due to the presence of nonlinearities. Indeed, Z_{IN} is a function of the oscillating signal frequency, RF frequency and power level, and current level of the ideal current source. Under steady state condition, the voltage across the break point will be zero as required and the driving current is the actual current flowing through that circuit path. Thus, with the frequency-dependent Z_S, the SOM analysis is conveniently reduced to a problem dealing only with the oscillating signal.

The SOM problem can be sub-divided into two separate states: 1) idle state, and 2) mixing state. The idle state represents the condition of the SOM without the presence of RF signal while the mixing state represents that with the presence of a RF signal.

Manuscript received April 9, 1995; revised November 12, 1995. This work was supported in part by US Army Research Office Contract DAAH04-93-G-0068 and by the Joint Services Electronics Program F49620-92-C-0055.

The authors are with the Department of Electrical Engineering, University of California, Los Angeles, CA 90095 USA.

Publisher Item Identifier S 0018-9480(96)01449-4.

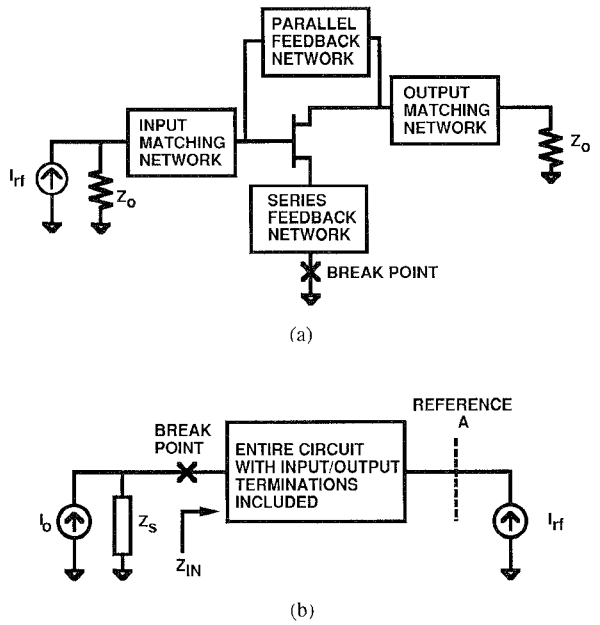

Fig. 1. Conversion of a circuit to a one-port network

A. Idle State

Without the presence of the RF, the nonlinear impedance can be represented by Volterra series as

$$Z_{\mathrm{IN}}(\omega_0, I_0) = Z_1(\omega_0) + 0.75Z_3(\omega_0, -\omega_0, \omega_0)|I_0|^2 + 0.625Z_5(\omega_0, -\omega_0, \omega_0, -\omega_0, \omega_0)|I_0|^4 + \cdots \quad (1)$$

where Z_1, Z_3, and Z_5 are the first-, third- and fifth-order impedance transfer functions. These functions represent the various orders V-I relationship at that artificially created port, due to the power-series type nonlinearities. One point to note is that Z_1 is the small-signal impedance and is expected to be negative over a range of frequencies. Thus, the problem is reduced to that of varying I_0 and ω_0 to match Z_{IN} to a short-circuit impedance.

B. Mixing State

In the presence of RF, the nonlinear impedance can be represented by Volterra series as

$$\begin{aligned} Z_{\mathrm{IN}}(\omega_0, I_0) &= Z_{1R}(\omega_0) + 0.75Z_{3R}(\omega_0, -\omega_0, \omega_0)|I_0|^2 \\ &+ 0.75Z_{3R}(\omega_{\mathrm{if}}, -\omega_{\mathrm{if}}, \omega_0)|I_{\mathrm{if}}|^2 \\ &+ 0.625Z_{5R}(\omega_0, -\omega_0, \omega_0, -\omega_0, \omega_0)|I_0|^4 \\ &+ 0.625Z_{5R}(\omega_{\mathrm{rf}}, -\omega_{\mathrm{rf}}, \omega_{\mathrm{rf}}, -\omega_{\mathrm{rf}}, \omega_0)|I_{\mathrm{rf}}|^4 \\ &+ 0.625Z_{5R}(\omega_{\mathrm{rf}}, -\omega_{\mathrm{rf}}, \omega_0, -\omega_0, \omega_0)|I_{\mathrm{rf}}|^2|I_0|^2 + \cdots \quad (2) \end{aligned}$$

where I_{if} is the RF current calculated from the available power equation for a given RF signal power. The available power equation is given as

$$P_{\mathrm{rf}} = \frac{1}{8} I_{\mathrm{rf}}^2 R \quad (3)$$

where R is the terminating resistance. This allows any impedance mismatch to be considered in the analysis. The transfer function in (2) is two-tone in nature with the presence of RF signal. They represent not only the various order of the nonlinear input impedances but also the nonlinear coupling impedances at the various ports for all desired frequencies. Looking at (1) and (2) show that only the magnitudes of I_{rf} and I_0 are required. There is a certain phase relationship between the RF and oscillating signals [12]. However, given the way this problem is formulated, no such information is required.

Once converges, the obtained value of I_0 and ω_0 are used to calculate the IF voltage, V_{if} across the load. V_{if} can then be represented as

$$\begin{aligned} V_{\mathrm{if}}(\omega_0, I_0, I_{\mathrm{rf}}) &= [0.5Z_{2R}(\omega_0, -\omega_{\mathrm{rf}}) + 0.75Z_{4R}(\omega_0, -\omega_0, \omega_0, -\omega_{\mathrm{rf}})|I_0|^2 \\ &+ 0.75Z_{4R}(\omega_{\mathrm{rf}}, -\omega_{\mathrm{rf}}, \omega_0, -\omega_{\mathrm{rf}})|I_{\mathrm{rf}}|^2 + \cdots]I_0 I_{\mathrm{rf}}^*. \quad (4) \end{aligned}$$

It can be seen in (4) that for the calculation of the IF power level, the phase relationship between I_0 and I_{rf} is also not required. It can also be shown that the phase relationship is not required for the calculation of the image and harmonic signals too. Since the phase relationships amongst the signals are not required, real-valued currents are used in this analysis for simplification.

III. Numerical Implementation

The algorithm adopted here is similar to that proposed in [11]. The algorithm involves varying two real-valued parameters, I_0 and ω_0 in the search for $Z_{\mathrm{IN}} = 0$. The steps of the algorithm are defined as follows:

1) Set $k = 0$ (where k is the iteration number) with $I_0^k = 1$ μA and ω_0^k approximately equal to that of the oscillation frequency derived from linear circuit analysis;
2) vary ω_0 until $|\mathrm{Im}[Z_{\mathrm{IN}}(\omega_0, I_0)]| < \varepsilon$, a pre-determined tolerance;
3) with ω_0^{k+1} obtained in step 2), a new I_0^{k+1} is calculated using the following (5) or (6), depending on the state of the SOM under consideration:

Idle State:

$$|I_0^{k+1}|^2 = -\mathrm{Re}[Z_1(\omega_0) + 0.625Z_5 \times (\omega_0, -\omega_0, \omega_0, -\omega_0, \omega_0)|I_0|^4 + \cdots]/\mathrm{Re}[0.75Z_3(\omega_0, -\omega_0, \omega_0)] \quad (5)$$

Mixing State:

$$\begin{aligned} |I_0^{k+1}|^2 &= -\mathrm{Re}[Z_{1R}(\omega_0) + 0.75Z_{3R}(\omega_{\mathrm{rf}}, -\omega_{\mathrm{rf}}, \omega_0)|I_{\mathrm{rf}}|^2 \\ &+ 0.625Z_{5R}(\omega_0, -\omega_0, \omega_0, -\omega_0, \omega_0)|I_0|^4 \\ &+ 0.625Z_{5R}(\omega_{\mathrm{rf}}, -\omega_{\mathrm{rf}}, \omega_{\mathrm{rf}}, -\omega_{\mathrm{rf}}, \omega_0)|I_{\mathrm{rf}}|^4 \\ &+ 0.625Z_{5R}(\omega_{\mathrm{rf}}, -\omega_{\mathrm{rf}}, \omega_0, -\omega_0, \omega_0) \\ &\times |I_{\mathrm{rf}}|^2|I_0|^2 + \cdots]/ \\ &\mathrm{Re}[0.75Z_{3R}(\omega_0, -\omega_0, \omega_0)]. \quad (6) \end{aligned}$$

Since the $\mathrm{Im}[Z_{\mathrm{IN}}]$ is zero at ω_0^{k+1}, as enforced in step 2, (1) or (2) are real-valued. Thus, (5) and (6) are

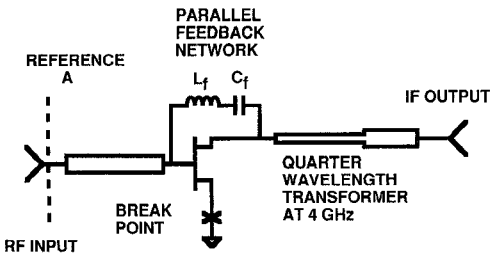

Fig. 2. Schematic diagram of the SOM.

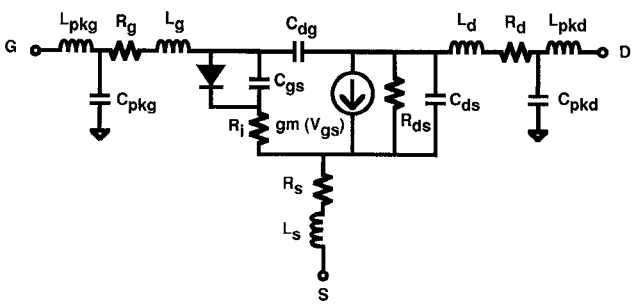

Fig. 3. Equivalent circuit of the MESFET.

derived by setting $\mathrm{Re}[Z_{\mathrm{IN}}]$ of (1) and (2), respectively, to zero and manipulating the real part of the (5) and (6) provides an update of I_0 which attempts to cause $\mathrm{Re}[Z_{\mathrm{IN}}] = 0$ given ω_0^{k+1}. However, this update can upset the condition $\mathrm{Im}[Z_{\mathrm{IN}}] = 0$ and further iteration is needed.

4) A further update of I_0 is made as follows

$$I_0^{k+1} = pI_0^{k+1} + (1-p)I_0^k \qquad \text{where } 0 < p < 1;$$

5) go to step 2) until

$$|Z_{\mathrm{IN}}(\omega_0^{k+1}, I_0)| < \gamma, \text{ a predetermined tolerance;}$$

6) compute all the output power level of desired frequencies.

The search subroutine in step 2) is taken from IMSL. A value of 2.5 is used for p in step 4). The transfer functions are derived using nonlinear current method [13]. This method is suitable for CAD applications and allows calculation of higher order transfer functions. A program capable of generating up to the seventh order transfer function has been developed. This allows strong nonlinearities to be represented using Volterra series. Details of this method will not be presented here as [14] provides a detailed discussion on this topic. The program also handles both states automatically. Since Z_{IN} is only a function of two variables, global convergence is not an issue. As in [11], the initial guess of the oscillating frequency is the resonant frequency approximated from linear analysis.

IV. Modeling and Design of SOM

To verify the approach proposed above, a simple oscillator/mixer circuit, as shown in Fig. 2, is used. The whole circuit is fabricated on Duroid substrate with $\varepsilon_r = 2.33$ and thickness 20 mils. The FET used in this circuit is a NEC71083. A LC series combination is used as a parallel feedback network across the gate and drain to provide negative resistance at about 6 GHz. A low Q quarter-wavelength transformer at 4 GHz is connected at the drain to provide proper matching impedance. In the analysis, the transformer is treated as ideal transmission line. HP11612A external bias network are used at each port to provide broadband biasing.

The FET is represented by an equivalent circuit as shown in Fig. 3. Package parasitics are included in the gate and drain. The value of the linear elements are derived through optimization using S-parameters of the FET biased at $V_{\mathrm{ds}} = 3$ V and $I_{\mathrm{ds}} = 30$ mA, over the 2–18 GHz frequency range obtained from catalog. TOUCHSTONE is used for this optimization step. The optimized values are tabulated in Table I. Since these linear elements do not vary significantly with bias, the obtained values are good for other bias condition close to that of $V_{\mathrm{ds}} = 3$ V and $I_{\mathrm{ds}} = 30$ mA.

TABLE I
Optimized Values of the Equivalent Circuit Parameters

OPTIMISED VALUE OF THE EQUIVALENT CIRCUIT PARAMETERS BIASED AT V_{ds} = 3 V and I_{ds} = 30 mA	
R_g (Ω)	0.21
R_s (Ω)	0.29
R_d (Ω)	1.52
R_i (Ω)	2.16
R_{ds} (Ω)	251
L_g (nH)	0.34
L_s (nH)	0.12
L_d (nH)	0.47
C_{gd} (pF)	0.04
C_{ds} (pF)	0.09
C_{gs} (pF)	0.39
C_{pkg} (pF)	0.21
C_{pkd} (pF)	0.25
L_{pkg} (nH)	0.16
L_{pkd} (nH)	0.19

Here, the two dominant nonlinearities, transconductance and gate diode characteristic, are considered. The nonlinearities of C_{gs} and C_{ds} are not considered. To simplify the problem, the effect of the drain voltage on the drain current is not considered, reducing the relationship to a one-dimensional polynomial. The DC I-V characteristics of the FET is measured on a HP4145A Semiconductor Parameter Analyzer. The load impedance looking out from the drain at the small-signal oscillating frequency is determined using the small-signal equivalent circuit of the FET. The calculated load is then used to generate a load-line, which is superimposed on the I-V characteristics. Variation of I_{ds} with respect to V_{gs} is then extracted and expanded into a power series about the desired DC bias point. As a compromise between oscillation and mixing conditions, the FET is biased at $V_{\mathrm{ds}} = 3$ V and $I_{\mathrm{ds}} = 25$ mA. The generated power series for I_{ds} is then

$$I_{\mathrm{ds}} = 61.61\ V_{\mathrm{gs}} + 33.23\ V_{\mathrm{gs}}^2 - 19.96\ V_{\mathrm{gs}}^3 - 14.62\ V_{\mathrm{gs}}^4 - 0.68\ V_{\mathrm{gs}}^5 \qquad (7)$$

where V_{gs} is in volts and I_{ds} is in mA.

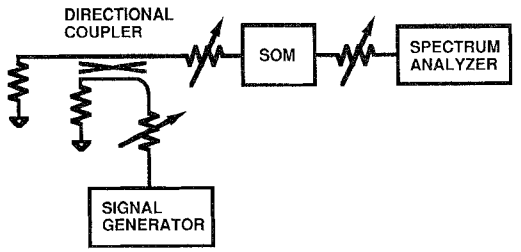

Fig. 4. Measurement setup

The gate-diode conduction characteristic is also measured on HP4145A with the drain open-circuited. The diode current is assumed to be that of an ideal Schottky diode and can be represented as

$$I_{gs} = I_{gs0}(e^{\alpha V_{gs}} - 1). \tag{8}$$

A parameter fit is made to match the measured data to the above equation with I_{gs0} and α being the unknowns. With fitted values of I_{gs0} and α, (8) is expanded as a Taylor series about the gate bias voltage and the derived polynomial is

$$I_{gs} = 2.04\ V_{gs} + 4.25\ V_{gs}^2 + 5.89\ V_{gs}^3 + 6.13\ V_{gs}^4 + 5.10\ V_{gs}^5 + 3.53\ V_{gs}^6 + \cdots \tag{9}$$

where V_{gs} is in volts and I_{gs} in mA.

V. Results

The measurement setup for the circuit is shown in Fig. 4. A 1.0–12.4 GHz coupler with 16 dB coupling is used to provide proper termination over the wide range of frequencies (RF, IF, and oscillating signals). The coupler also allows signals at the gate port to be measured. The output is then observed on a HP8562A Spectrum Analyzer, which has a frequency counter option. Attenuators are included to ensure proper termination. Calibration is made with a HP437B Power Meter at all relevant frequencies to account for the error in the spectrum analyzer, and cable and coupler insertion losses.

The SOM circuit is biased at $V_{ds} = 3$ V and $I_{ds} = 23.58$ mA. Initially, the SOM is left in the idle state. The measured frequency and power level of the oscillating signal and its associated second harmonic are shown in Table II. Theoretical prediction using Volterra series up to the fifth-order is also included for comparison. Calculation using seventh order transfer function shows no significant improvement in the results, indicating that convergence has been achieved. Fifth order is used so as to reduce the CPU time. The measured results show good agreement with that calculated. There is some discrepancy in the second harmonic power level. As observed in [11], this is because the nonlinearity of C_{gs} is not taken into account.

Next, the SOM under mixing state is measured. A HP8350B generator is used to provide the RF signal. The RF signal power level at reference plane A indicated at Fig. 2 is first measured with HP347B to obtain the available power level. (3) is then used to calculate the I_{rf}. Measurements made at the gate port show that the performance of the SOM is poorer compared to that at the drain. Thus, only measured results at the drain will be reported.

TABLE II
Measured and Calculated Performance of the SOM in Idle State

	CALCULATED	MEASURED
FUNDAMENTAL OSCILLATION FREQUENCY (GHz)	5.901	5.894
FUNDAMENTAL SIGNAL POWER LEVEL (dBm)	12.7	13.4
SECOND HARMONIC POWER LEVEL (dBm)	-10.6	-6.6

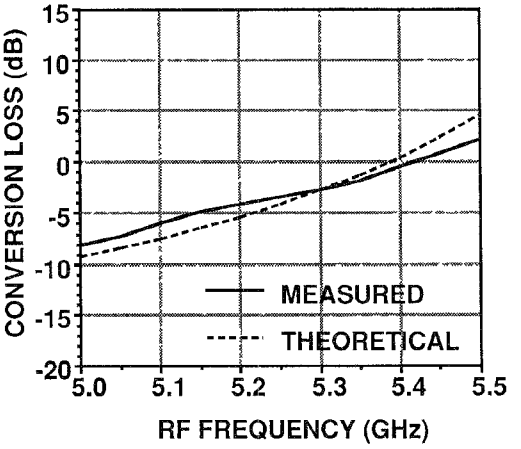

Fig. 5. Measured and calculated conversion loss/gain of the SOM with respect to RF frequency.

The conversion loss/gain of the SOM is first measured with a RF frequency sweep between 5.0 and 5.5 GHz with a step of 0.05 GHz. The conversion loss is calculated with reference to the available RF power. The input RF available power level is set to -18 dBm at reference plane A in Fig. 1(b). The measured and calculated conversion loss/gain is shown in Fig. 5. Again, fifth order Volterra series is used to save CPU time. The agreement is better than 1 dB over most of the frequency band. The discrepancy is greater when the RF frequency is closer to that of the oscillating frequency. This is because in the neighborhood of the oscillating frequency, there is negative resistance. This provides some form of amplification for the RF signal. Thus, the system becomes strongly nonlinear as there are two strong signals present.

As the mixing process takes place, it is expected that the oscillating signal power level to be lowered due to the conservation of power. Also, some frequency pulling is expected. Figs. 6 and 7 show respectively the variation of oscillating signal power and frequency shift with respect to the RF frequency variation. Frequency shift is taken relative to the oscillating frequency in the idle state. The discrepancy in the power variation between measured and that calculated

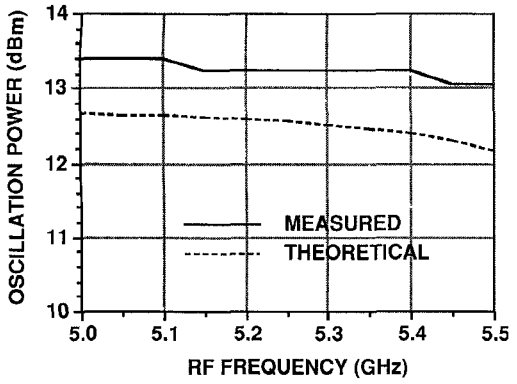

Fig. 6. Measured and calculated oscillating power of the SOM with respect to RF frequency.

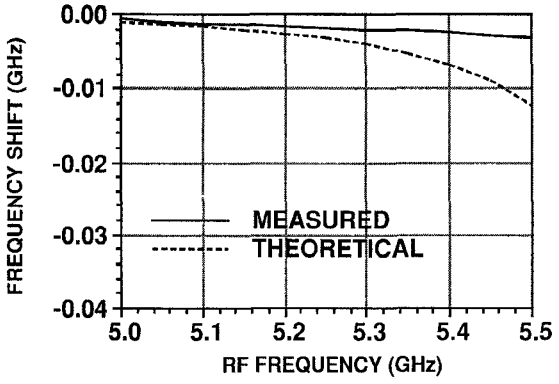

Fig 7. Measured and calculated oscillating frequency shift of the SOM with respect to RF frequency.

is within 2 dB. However, there is some discrepancy in the frequency drift as the RF frequency approaches that of the oscillating frequency. Again, this is due to the fact that the system is now highly nonlinear. But, the theory does predict correctly the trend of variation.

Lastly, the SOM is measured with a RF signal at 5.3 GHz. The RF available power is varied between -18 dBm to -8 dBm in step of 1 dBm. The measured variation of conversion loss/gain and oscillating frequency shift with respect to RF power are shown in Figs. 8 and 9 respectively. The theoretical results are also in good agreement with measurement up to a RF power of about -12 dBm. This is because as the RF power increases, the system becomes highly nonlinear and other nonlinearities are now expected to have significant effect on the mixing process. However, the theory does predict the trend of saturation well in the conversion loss/gain.

VI. Conclusion

A new approach to the problem of self-oscillating mixer has been made using Volterra series. The advantage of this method is that the phase relationship between the RF and oscillating signals is not required in the formulation of the problem. Also, the stability criterion is not needed for convergence test to a correct solution numerically. Nonlinear current method is used to generate the kernels, resulting in its ability to generate higher-order kernels. This means that strong nonlinearities can be represented and that the approach is compatible to

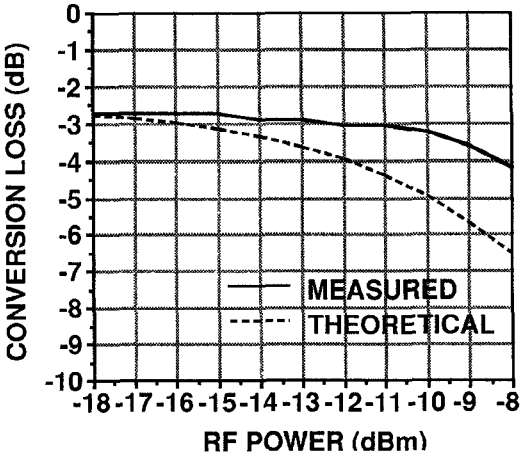

Fig. 8. Measured and calculated conversion loss/gain of the SOM with respect to RF power.

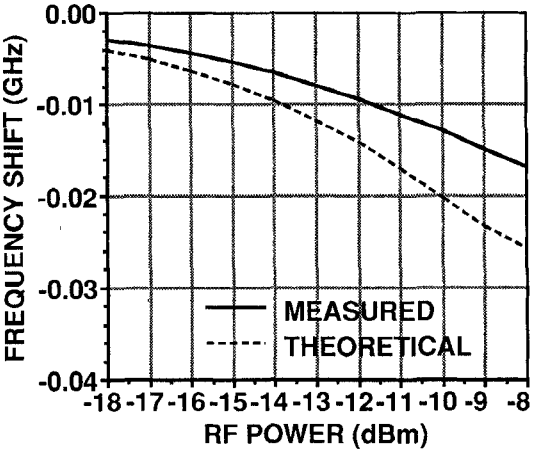

Fig. 9. Measured and calculated oscillating frequency shift of the SOM with respect to RF power.

CAD. Convergence is ensured as the initial guess is derived from small-signal analysis. Although the FET equivalent circuit used here is simple, the theoretical results are in good agreement with that measured with RF frequency and power sweeps. This approach is not restricted to this FET model and more complete nonlinear equivalent circuit can be used.

Acknowledgment

The authors would like to thank M. Christianson and M. Espiau of the Center of High Frequency Eletronics, University of California at Los Angeles, for their assistance in measurement and fabrication of the circuit.

References

[1] V. D. Hwang and T. Itoh, "Quasi-optical HEMT and MESFET self-oscillating mixers," in *1988 IEEE MTT-S Int. Microwave Symp. Dig.*, May 1988, pp. 25–27.

[2] G.-W Wang, T.-J. Lin, and S.-Y. Yang, "A low cost DBS low noise block downconverter with a DR stabilized MESFET self-oscillating mixer," in *1994 IEEE MTT-S Int. Microwave Symp. Dig.*, May 1994, pp. 1447–1450.

[3] C. Toker, "Self-oscillating tunnel-diode mixer having conversion gain," *IEEE Trans. Microwave Theory and Tech.*, vol. MTT-20, pp. 616–618, Sept. 1972.

[4] M. Claassen and U. Güttich, "Conversion matrix and gain of self-oscillating mixers," *IEEE Trans. Microwave Theory and Tech.*, vol. 39, pp. 25–30, Jan. 1991.
[5] I. Kipnis and A. S. Khanna, "Large-signal computer-aided analysis and design of silicon bipolar MMIC oscillators and self-oscillating mixers," *IEEE Trans. Microwave Theory Tech.*, vol. 37, pp. 558–564, Mar. 1989.
[6] V. Rizzoli and A. Neri, "Harmonic-balance analysis of multitone autonomous nonlinear microwave circuits," in *1991 IEEE MTT-S Int. Microwave Symp. Dig.*, May 1991, pp. 107–110.
[7] T. Endo and L. O. Chua, "Quasi-periodic oscillation via volterra series," in *1986 IEEE Int. Symp. Circuits Syst. Dig.*, May 1986, pp. 57–60.
[8] J. J. Bussgang, L. Ehrman, and J. W. Graham, "Analysis of nonlinear systems with multiple inputs," in *Proc. IEEE*, Aug. 1974, vol. 62, no. 8, pp. 1088–1117.
[9] S. Narayanan, "Transistor distortion analysis using volterra series representation," *Bell Syst. Tech. J.*, pp. 991–1025, May–June 1967.
[10] C.-C. Huang and T.-H. Chu, "Analysis of MESFET injection-locked oscillators in fundamental mode of operation," *IEEE Trans. Microwave Theory Tech.*, vol. 42, pp. 1851–1857, Oct. 1994.
[11] K. K. M. Cheng and J. K. A. Everard, "A new and efficient approach to the analysis and design of GaAs MESFET microwave oscillators," in *1990 IEEE MTT-S Symp. Dig.*, 1990, pp. 1283–1286.
[12] M. Armand, "On the output spectrum of unlocked driven oscillators," in *Proc. IEEE*, May 1969, pp. 798–799.
[13] S. A. Mass, "A general-purpose computer program for the volterra-series analysis of the nonlinear microwave circuits," in *1988 IEEE MTT-S Int. Microwave Symp. Dig.*, May 1988, pp. 311–314.
[14] ——, *Nonlinear Microwave Circuits*. Norwood, MA: Artech House, 1988.

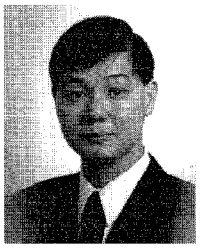

Siou Teck Chew (S'94) was born in Singapore on November 3, 1964. He received the B.Eng. and M.Eng. from National University of Singapore, Singapore, in 1989 and 1993, respectively. Currently, he is working toward a Ph.D. at the University of California, Los Angeles.

Since 1989, he has worked for the Defence Science Organization, Singapore, as a Research Engineer in microwave circuit designs. His current research interests include active antenna design, nonlinear circuit analysis and filter designs.

Tatsuo Itoh (S'69–M'69–SM'79–F'82) received the Ph.D. degree in electrical engineering from the University of Illinois, Urbana in 1969.

From 1966 to 1976, he was with the Electrical Engineering Department, University of Illinois. From 1976 to 1977, he was a Senior Research Engineer in the Radio Physics Laboratory, SRI International, Menlo Park, CA. From 1977 to 1978, he was an Associate Professor at the University of Kentucky, Lexington. In July 1978, he joined the faculty at The University of Texas at Austin, where he became a Professor of Electrical Engineering in 1981 and Director of the Electrical Engineering Research Laboratory in 1984. During the summer of 1979, he was a guest researcher at AEG-Telefunken, Ulm, West Germany. In 1983, he was selected to hold the Hayden Head Centennial Professorship of Engineering at The University of Texas. In 1984, he was appointed Associate Chairman for Research and Planning of the Electrical and Computer Engineering Department at The University of Texas. In 1991, he joined the University of California, Los Angeles as Professor of Electrical Engineering and holder of the TRW Endowed Chair in Microwave and Millimeter Wave Electronics. He is currently Director of Joint Services Electronics Program (JSEP) and is also Director of Multidisciplinary University Research Initiative (MURI) program at UCLA. He was an Honorary Visiting Professor at Nanjin Institute of Technology, China, and at the Japan Defense Academy. In 1994, he was appointed Adjunct Research Officer for Communications Research Laboratory, Ministry of Post and Telecommunication, Japan. He currently holds Visiting Professorship at University of Leeds, United Kingdom. He has more then 200 journal publications, 350 refereed conference presentations in the area of microwaves, millimeter-waves, antennas, and numerical electromagnetics. He has generated more than 30 Ph.D. students.

Dr. Itoh is a Fellow of the IEEE, a member of the Institute of Electronics and Communication Engineers of Japan, and Commissions B and D of USNC/URSI. He served as the Editor of IEEE TRANSACTIONS ON MICROWAVE THEORY AND TECHNIQUES for 1983–1985. He serves on the Administrative Committee of IEEE Microwave Theory and Techniques Society. He was Vice President of the Microwave Theory and Techniques Society in 1989 and President in 1990. He was the Editor-in-Chief of IEEE MICROWAVE AND GUIDED WAVE LETTERS from 1991 through 1994. He was elected as an Honorary Life Member of MTT Society in 1994. He was the Chairman of USNC/URSI Commission D from 1988 to 1990, the Vice Chairman of Commission D of the International URSI for 1991 through 1993 and is currently Chairman of the same Commission. He serves on advisory boards and committees of a number of organizations including the National Research Council and the Institute of Mobile and Satellite Communication, Germany.